J Mol Model
DOI 10.1007/s00894-011-1061-0

ORIGINAL PAPER

Tetrahydroisoquinolines acting as dopaminergic ligands. A molecular modeling study using MD simulations and QM calculations

Sebastián Andujar · Fernando Suvire · Inmaculada Berenguer · Nuria Cabedo · Paloma Marín · Laura Moreno · María Dolores Ivorra · Diego Cortes · Ricardo D. Enriz

Received: 15 December 2010 / Accepted: 22 March 2011

Abstract A molecular modeling study on 16 1-benzyl tetrahydroisoquinolines (BTHIQs) acting as dopaminergic ligands was carried out. By combining molecular dynamics simulations with ab initio and density functional theory (DFT) calculations, a simple and generally applicable procedure to evaluate the binding energies of BTHIQs interacting with the human dopamine D2 receptor (D2 DR) is reported here, providing a clear picture of the binding interactions of BTHIQs from both structural and energetic viewpoints. Molecular aspects of the binding interactions between BTHIQs and the D2 DR are discussed in detail. A significant correlation between binding energies obtained from DFT calculations and experimental p*Ki* values was obtained, predicting the potential dopaminergic effect of non-synthesized BTHIQs.

Keywords 1-Benzyl-THIQ · Halogenated-1-benzyl-THIQ · D2-dopamine receptor · Structure-activity relationship · Molecular dynamic simulation · Ab initio and DFT calculation

S. Andujar · F. Suvire · R. D. Enriz (✉)
Departamento de Química, Universidad Nacional de San Luis, San Luis, Argentina
e-mail: denriz@unsl.edu.ar

S. Andujar · R. D. Enriz
IMIBIO-SL (CONICET),
Chacabuco 915,
5700, San Luis, Argentina

I. Berenguer · N. Cabedo · P. Marín · L. Moreno · M. Dolores Ivorra · D. Cortes
Departamento de Farmacología, Facultad de Farmacia, Universidad de Valencia,
46100 Burjassot Valencia, Spain

Introduction

The dopamine D2 receptor (D2 DR) has been implicated in the mechanism of drugs used in the treatment of disorders such as schizophrenia and Parkinson's disease. For these reasons, a great deal of research has focused on the discovery of novel dopaminergic ligands as potential drug candidates [1]. DR can be classified into two pharmacological families (D1 and D2-like) that are encoded by at least five genes. Which receptor(s) needs to be activated to obtain therapeutic effects in Parkinson's disease has been the subject of controversy [2]. The D2-like DR show high affinities for drugs (antagonists) used in the treatment of schizophrenia (antipsychotics) and those (agonists) utilized to treat the Parkinson's disease [3].

Tetrahydroisoquinolines (THIQs)—the most numerous naturally occurring alkaloids—include 1-benzyl-THIQs and aporphines, both of which have structural similarities to dopamine and can interact with DR [4]. Previous results in our group suggested that some natural and synthetic 1-benzyl-THIQs alkaloids were able to bind to DR [5–7]. In this way, we described the enantioselective syntheses of pairs of dopaminergic (1*S*)- and (1*R*)-benzyl-THIQs using (*R*)- and (*S*)-phenylglycinol as the chiral source, and we observed that, in these series of 1-benzyl-THIQs, (1*S*)-enantiomers were 5–15 times more effective at D1-like and D2-like dopamine receptors than (1*R*)-enantiomers [8] (Fig. 1). On the other hand, we described the preparation in a 'one-pot' sequence of 1-cyclohexylmethyl 7,8-dioxygenated-THIQ, substituted and unsubstituted in the C ring by application of the photo–Fries transposition, followed by a tandem reduction-cyclization and further reduction. Indeed, we accomplished for the first time a regioselective hydrogenation of the benzyl ring in the THIQ system. All 1-cyclohexylmethyl THIQs studied in

Published online: 27 April 2011

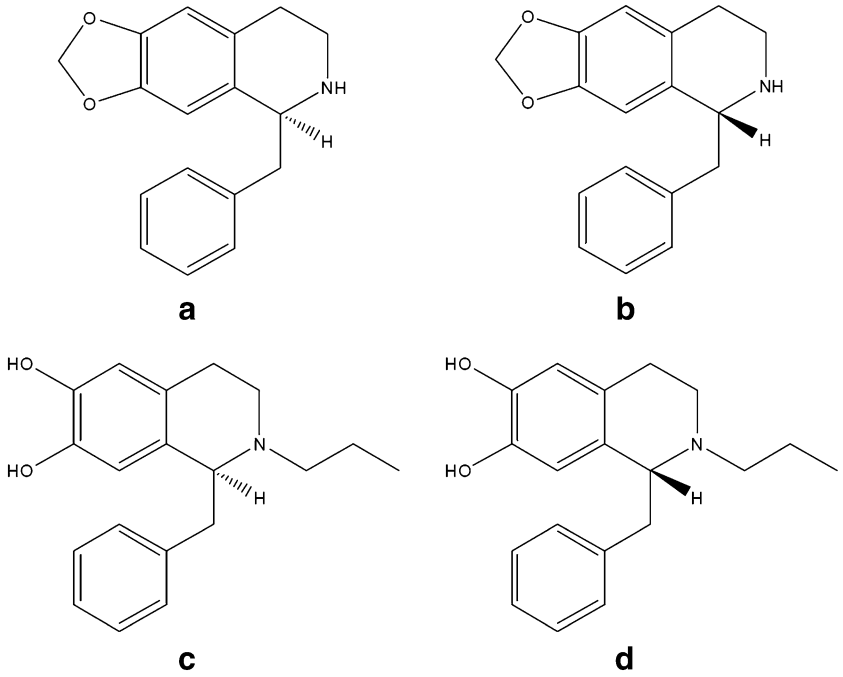

Fig. 1 **a**–**d** Structural features of tetrahydroisoquinoline (THIQ) compounds. **a** (1S)-1-Benzyl-6,7-methylenedioxy-1,2,3,4-THIQ. **b** (1R)-1-Benzyl-6,7-methylenedioxy-1,2,3,4-THIQ. **c** (1S)-N-Propyl-1-benzyl-6,7-dihydroxy-1,2,3,4-THIQ. **d** (1R)-N-Propyl-1-benzyl-6,7-dihydroxy-1,2,3,4-THIQ (previously reported in [8])

this work were able to displace the D2-like DR radioligand from its specific binding sites in rat striatal membranes, while the *N*-methylated derivatives also showed affinity for the D1-like DR. Recently, we reported the influence of the substitution at the 1-position over a 7-chloro-6-hydroxy-THIQ core [9, 10]. In previous works [8, 11–15], we determined the role of certain structural requirements for improving the affinity for D1 and D2-like DR. Thus, we are able to postulate that the presence of a hydroxyl (OH) and a halogen group (Cl) in the THIQ A-ring could lead to obtaining molecules that can bind selectively to one of the two groups of receptors mentioned above [13, 14]. Preserving the chlorine and hydroxyl (or methoxyl) groups at the C-6 and C-7 positions of the THIQ A-ring, respectively, with a secondary (*N*H) or a tertiary (*N*Me) amine, we explored the impact of inclusion of aliphatic and aromatic groups such as butyl-, phenyl-, benzyl-[8] as well as halogenated-1-benzylbenzyl moieties at 1-position [9] to determine their influence over dopaminergic activity. Thus, we have recently reported five series of 1-substituted-THIQs: 1-butyl-THIQs (compounds **1**–**3** in Fig. 2), 1-phenyl-THIQs (**4**–**6**), 1-benzyl-THIQs (**7**–**9**), 2′-bromobenzyl-THIQs (**11**–**13**) and 2′,4′-dichlorobenzyl-THIQs (**14**–**16**). Compound **10**, which was obtained from a fortuitous synthesis, was also included in such a report [8]. During a Bischler-Napieralski cyclization, we observed the same fact reported by Doi et al. in 1997 [16] when preparing 1-butyl-THIQs. The need to add P_2O_5 (and $POCl_3$ at a molar ratio of 1:1) to the cyclodehydration reaction, because of the difficulty of cyclizing the amide when there is a chlorine in the structure (originally at the C-6 position of the A-ring), causes an aberrant cyclization, by means of formation of a nitrilium intermediate, which gives two positional isomers, clearly identified after the reduction step: 6-chloro-7-hydroxy-1-butyl-THIQ (compound **2**), and 6-hydroxy,7-chloro-1-butyl-THIQ (compound **10**: unexpected cyclization product), in a 1:2 ratio.

All these compounds were assayed in vitro for their ability to displace selective radioligands of D1 and D2 DR from their respective specific binding sites in rat striatal membranes, and were tested for their ability to inhibit in vitro ^{3}[H]-dopamine uptake in rat striatal synaptosomes. Many of these compounds were able to displace both ^{3}[H]-SCH 23390 and ^{3}[H]-raclopride at nano or micromolar (nM or μM) concentration from their specific binding sites in rat striatum, but all compounds had only low or no effect on ^{3}[H]-dopamine uptake [8, 9]. The replacement at the C-1 position of THIQs, is an important factor modulating the selectivity at DR. Compounds **1**, **3**, **10** and **11** (Table 1) show a greater affinity towards D2 receptors when a butyl or a benzyl moiety, respectively, is located in that position. The different activities and selectivity obtained for these compounds can be explained by the different spatial orientations adopted by the varied hydrophobic portions located at C-1, which could give different molecular interactions with the D1 and D2 receptors. Since some BTHIQs have shown a great affinity for the D2 DR, considerable interest has developed in delineating the portions of the BTHIQ molecular structure responsible for its dopaminergic properties and interactions with the D2 DR. The process of drug design could be considerably improved if receptors and their mode of interaction with ligands were known in precise molecular detail. Such

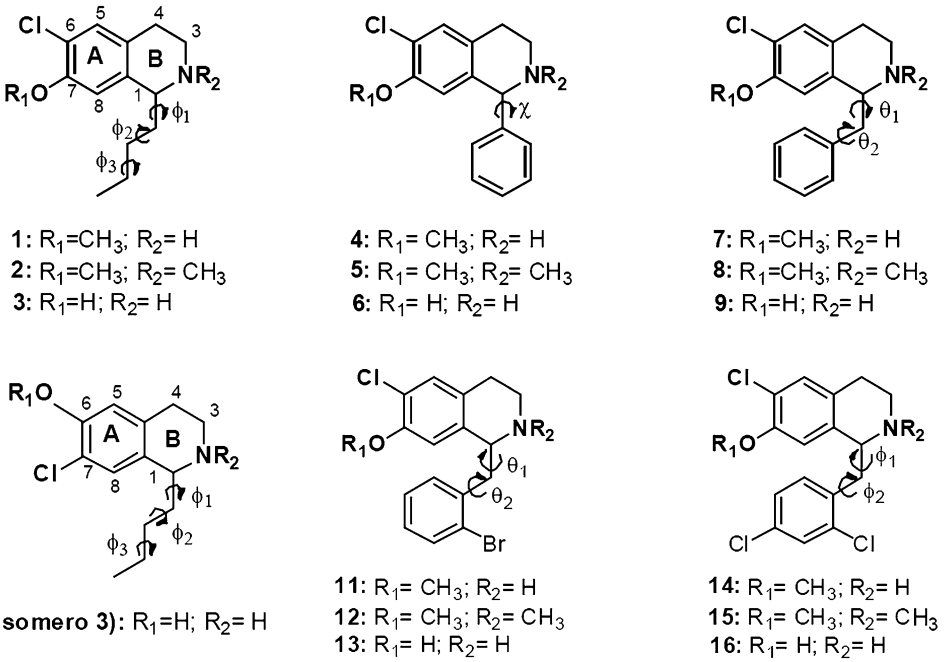

Fig. 2 Structural features of the 16 BTHIQs reported here, showing the different torsional angles

information could then be used to design more defined structures in which the pharmacophoric groups are oriented in the appropriate spatial arrangement for optimal receptor interaction.

In the present work, we report a molecular modeling study performed on 16 BTHIQs acting as dopaminergic ligands. Combined molecular dynamics (MD) simulations and quantum mechanics (semiempirical, ab initio and DFT) calculations were employed in our study to evaluate the molecular interactions between the BTHIQs and the D2 DR. An excellent correlation between binding energies obtained from DFT calculations and experimental p*K*i was obtained.

Materials and methods

Theoretical calculations were carried out in two steps. In a first step, we performed MD simulations of the molecular

Table 1 Relative binding energies obtained for the different complexes. Previously reported experimental p*K*i data are shown in the last column

Compound	Relative binding energy (BE) (kcal/mol)				Specific-D2 ligand [^{3}H]-raclopride
	EU (RHF/6-31G(d))	Δ EU (RHF/6-31G(d))	EU (B3LYP/6-31G(d,p))	Δ EU (B3LYP/6-31G(d,p))	p*K*i
1	-98.91	22.16	-114.29	24.58	6.108±0.165 [9]
2	-80.00	41.07	-93.62	40.25	5.424±0.026 [9]
3	-111.92	9.15	-135.43	3.44	7.117±0.151 [9]
4	-75.46	45.61	-94.89	43.98	5.212±0.124 [9]
5	-83.02	38.05	-103.00	35.87	5.670±0.406 [9]
6	-90.48	30.59	-105.35	33.52	5.950±0.198 [9]
7	-99.94	21.13	-118.48	20.39	6.014±0.049 [9]
8	-84.29	36.78	-99.93	38.94	5.816±0.181 [9]
9	-116.35	4.72	-137.83	1.04	7.178±0.091 [9]
10	-114.03	7.04	-138.43	0.44	7.220±0.139 [9]
11	-100.47	20.6	-128.07	10.8	6.630±0.092 [10]
12	-81.59	39.48	-113.31	25.56	5.896±0.099 [10]
13	-121.07	0	-138.87	0	7.391±0.139 [10]
14	-74.61	46.46	-101.31	37.56	5.507±0.105 [10]
15	-77.31	43.76	-101.10	37.77	5.230±0.096 [10]
16	-102.79	18.28	-131.14	7.73	6.996±0.105 [10]

interactions between compounds **1**–**16** and D2 DR. In the second step, reduced model systems were optimized using quantum mechanics calculations. Semiempirical (AM1) combined with ab initio [RHF/6-31G(d)] and B3LYP [6-31G(d,p)] calculations were employed in these optimizations.

Molecular dynamics simulations

It must be pointed out that the principal goal of the MD simulations performed here was not to obtain a new D2 DR by homology. Our aim in this study was less ambitious; we wished to obtain a reasonable indication of the relationship between the structures of compounds **5**–**7** and their potential affinities for the binding pocket of D2 DR. Thus, for this purpose, we considered it more appropriate to use a previously reported and extensively tested model for D2 DR [17]. In fact, there are many molecular modeling studies in the literature reporting D2 DRs obtained by homology, all of them structurally closely related [18–20]. Thus, in the present study, we used the D2DR model previously reported in reference [17]. The ligand topologies were built using the mktop program [21]. For this purpose, we used the previously optimized geometry at RHF/6-31G (d) level of theory of the global minimum of each ligand. In the present study, we used an approach where manual docking was guided by information from site-directed mutagenesis and short docking simulations, with both the receptor and the ligand free to move. Structurally similar parts of the ligands were oriented in similar positions in the receptor model, which was described by Mansour et al. [22] and Lan et al. [23]. Thus, receptor–ligand complexes were prepared in order to obtain the input files for MD runs. Several docking positions were considered and the strongest receptor interactions were examined in detail.

The MD simulations and analysis were performed using the GROMACS 3.2.1 simulation package [24, 25] with the OPLS-AA force field [26–30] and the rigid SPC water model [31, 32] in a cubic box with periodic boundary conditions. Receptor–ligand complexes were embedded in a box containing the SPC water model that extended to at least 1 nm between the receptor and the edge of the box, resulting in a box of 7.17 nm in side length. The total number of water molecules was 11,330 for the different simulations. Three Na^+ ions were then added to the systems by replacing water in random positions, thus making the whole system neutral. The time step for simulations was 0.001 ps for a complete simulation time of 5 ns. For long-range interactions, the particle-mesh Ewald (PME) [33–35] method was used with a 1 nm cut-off and a Fourier spacing of 0.12 nm. The MD protocol consisted of several preparatory steps: energy minimization using the conjugate gradient model [36, 37] density stabilization (NPT conditions), and finally production of the MD simulation trajectory. All production simulations were performed under NVT conditions at 310 K, using Berendsen's coupling algorithm [38] for keeping the temperature constant. The compressibility was 4.8×10^{-5} bar^{-1}. All coordinates are saved every 5 ps. The SETTLE [24] algorithm was used to keep water molecules rigid. The LINCS [39] algorithm was also used to constrain all C-α atom positions for the receptor in order to avoid unfolding problems. The simulations were analyzed using the analysis tools provided in the Gromacs package.

Histidine in the active site is a potential problem because the state of His (neutral or protonated) is a controversial topic. We were particularly interested in performing simulations under physiological conditions (pH≈7). Previous reports have indicated that, under physiological conditions (pH≈7), histidine located in a hydrophobic environment (hydrophobic pocket without water molecules) is in neutral form [40]. In addition, previous simulations performed for D3DR by Micheli et al. [20] also considered the histidine residue to be neutral. Thus, on the basis of these results, we considered His in neutral form in our calculations. This amino acid was calculated as follow: protons were added using the program pdb2gmx, in the GROMACS suite of programs, for optimization of the hydrogen bond network. His protons were placed by default; these selections were done automatically (His was in neutral form). This is based on an optimal hydrogen bonding conformation. Hydrogen bonds are defined based on simple geometric criteria, specified by the maximum hydrogen–donor–acceptor angle and donor–acceptor distance.

It should be noted that the compounds reported here possess one chiral center, and are therefore enantiomeric with the possibility of two isomers (*1-S* and *1-R*). However, we did not perform an enantiomeric resolution for previously reported biological assays; thus, only one isomer of each compound was evaluated in our MD simulations. To choose the isomeric forms of each compound, we considered on the one hand previously reported results [15] and, on the other, preliminary and specially performed exploratory simulations determining the spatially preferred form of each compound (results not shown). Our previous experimental results on structurally related compounds suggested that the *S* form would be the preferred isomer for these compounds [15]. The preliminary and exploratory MD simulations are in agreement with these experimental data, indicating that the spatial ordering adopted by *1-S* forms gives adequate orientation of the molecules to interact in the active site of the dopamine D2 receptor.

The equilibrium state of the complexes was observed from the onset of simulation until 5 ns. The temperature was stabilized at 310±4 K for all complexes. The potential energy stabilized in a short time period (around 0.5 ns), and

the values obtained suggested that the system was well equilibrated.

Considering the 5 ns of MD simulation, and from the time profiles, it was concluded that some properties of the ligand–receptor complexes reached stable average values at around 0.5 ns, whereas others take longer time periods. For this reason, and to ensure full equilibration, only the last 4.5 ns were taken into account for the analysis. After discarding the first 0.5 ns of the trajectory, we followed the changes in spatial ordering of the ligand–receptors complexes.

Quantum mechanics calculations

The binding pocket of the D2 L–R (ligand-receptor) was defined according to Teeter et al. [41] and Neve et al. [42]. In our reduced model system, only 13 amino acids were included in molecular simulations. The size of the molecular system simulated and the complexity of the structures under investigation restricted the choice of the quantum mechanical method to be used. Consequently, the semiempirical AM1 method was selected combined with ab initio calculations (RHF/6-31G(d)). The torsional angles of the ligands and the flexible side-chains of the amino acids as well as the bond angles and bond lengths of the moieties involved in the potential intermolecular interactions were optimized at the semiempirical level. Next, the torsional angles of the ligands and the flexible side-chains of the amino acids as well as the potential intermolecular interactions were optimized at RHF/6-31G(d) and DFT [B3LYP/6-31G(d,p)] levels of theory. In contrast, the torsional angles of backbones as well as the bond angles and bond lengths of non-interacting residues were kept frozen during the calculations.

The binding energy of the complexes was calculated, with the approximation neglecting the superimposition of error due to the difference between the total energies of the complex with the sum of the total energies of the components:

$$BE_{QM}=E_{L/D2DR}-(E_{D2DR}+E_{L}) \quad (1)$$

where BE_{QM} is the binding energy, $E_{L/D2DR}$ is the complex energy, E_{D2DR} the energy of the reduced receptor model (binding pocket) and E_L the energy of the ligand.

All the quantum mechanical calculations reported here were carried out using the Gaussian 03 program [43].

Spatial views shown in Figs. 3, 9 and 10 were constructed using the UCSF Chimera program [44] as the graphic interface.

Results and discussion

Our molecular modeling study was carried out in two steps. First, we performed MD simulations of the molecular interactions between the compounds shown in Fig. 2 with the human D2 DR (Fig. 3). In the second step, reduced model systems (shown as a circle in Fig. 3) were optimized using quantum mechanic calculations. Semiempirical (AM1) combined with ab initio [RHF/6-31G(d)] and DFT [B3LYP/6-31G(d,p)] calculations were employed for these optimizations.

Molecular dynamic simulations

Comparing the results obtained for the different complexes led to interesting general conclusions. Consistent with previous experimental [22] and theoretical [45] results, our simulations indicate the importance of the negatively charged aspartate 86 for binding of these ligands. A highly conserved aspartic acid (Asp 86) in trans-membrane helix 3 (TM3) is important for the binding of both agonists and antagonists to the D2 receptor, [22, 46, 47], and its terminal carboxyl group may function as an anchoring point for ligands with a protonated amino group [23, 41, 42, 47]. In the present study, all the compounds simulated were docked into the receptor with the protonated amino group near Asp 86. After 5 ns of MD simulations, the ligands had moved slightly but in a different form compared with the initial position. However, the strong interaction with Asp 86 was maintained for all complexes (see Fig. 4), supporting the suggestion that Asp 86 functions as an anchoring point for ligands with a protonated amino group.

Pharmacological data [22, 48] indicate that the hydroxyl groups of dopaminergic ligands are of primary importance in stabilizing binding, suggesting that the serine residues (141 and 144) of the D2 receptor may not be equally important for binding affinity. Individual mutation of serines 141 and 144 in TM5 to alanine produced asymmetrical effects on dopamine receptor binding. These results indicated that Ser 141 might be differentially important for dopamine binding. In addition, site-directed mutagenesis studies have indicated that a cluster of serine residues in TM5 (Ser 141, Ser 144) and in TM4 (Ser 122 and Ser 118) is important for agonist binding and receptor activation [45, 47–49]. It was suggested that the serine cluster and dopamine form a hydrogen-bonding network. Such a hydrogen-bonding network was reproduced by the MD simulation of these complexes (Fig. 5). In these complexes, the strongest contributor to the network was Ser 141, which is consistent with the experimental observation that a Ser 141 Ala mutated receptor completely lost dopamine-induced activation [22]. The 7-hydroxyl group of compound **3** displayed another significant hydrogen bond interaction with Ser 122; however, this interaction is weaker with respect to the hydrogen bond with Ser 141.

Figure 5 shows that compounds **3** and **9** display strong hydrogen bond interactions with Ser141 during the entire

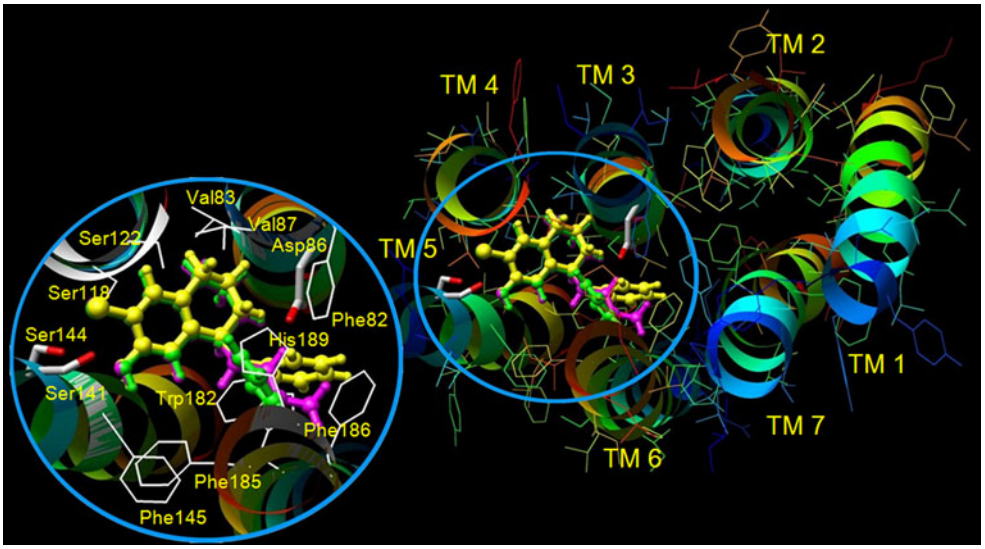

Fig. 3 Spatial view obtained for the dopamine D2 receptor (D2 DR) model. The plot was performed using the UCSF Chimera program [44] program as a graphic interface. Conformations used as starting geometries for the molecular dynamics (MD) simulations of compounds **3** (*cyan*), **6** (*green*) and **9** (*yellow*) are shown. The binding pocket optimized from quantum mechanics calculations is denoted with a *circle*. The numbers of the amino acids included correspond to reference [17] and not to those given in the crystal data

simulation period. Similar results were obtained for compounds **6**, **10**, **13** and **16**. However, for the rest of the BTHIQs evaluated here, such interactions were slightly weaker. It should be noted that in compounds **3**, **6**, **9**, **10**, **13** and **16**, the hydroxyl group on the ring-A is acting as a proton-donor; whereas the oxygen atom of the OH group of Ser141 is the proton-acceptor counterpart. In contrast, in the case of compounds **1**, **2**, **4**, **5**, **7**, **8**, **11**, **12**, **14** and **15**, the OH group of Ser 141 is the proton-donor and the methoxyl group on the ring-A is the acceptor counterpart. MD simulations predict that these interactions are weaker in comparison to those observed for hydroxyl ligands on the ring-A.

Aromatic side chains are bulky, have low barriers for rotation, and are ideal for adjusting to the changing conformation of the hydrophobic moiety of the ligand. In

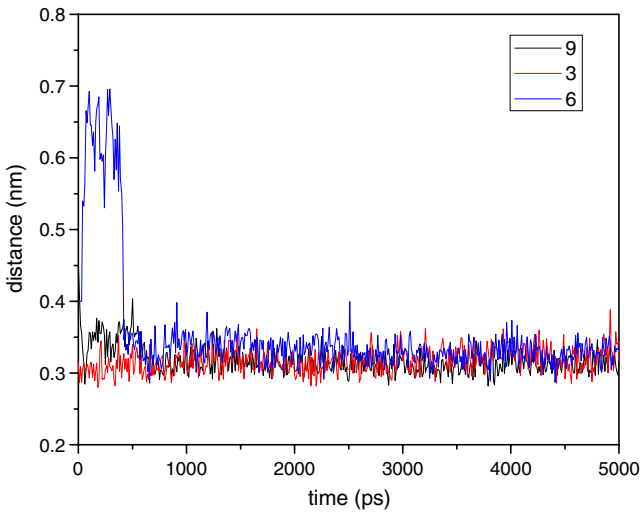

Fig. 4 Bond lengths obtained for the salt bridge between Asp 86 and the protonated amine group in compounds **3**, **6** and **9**

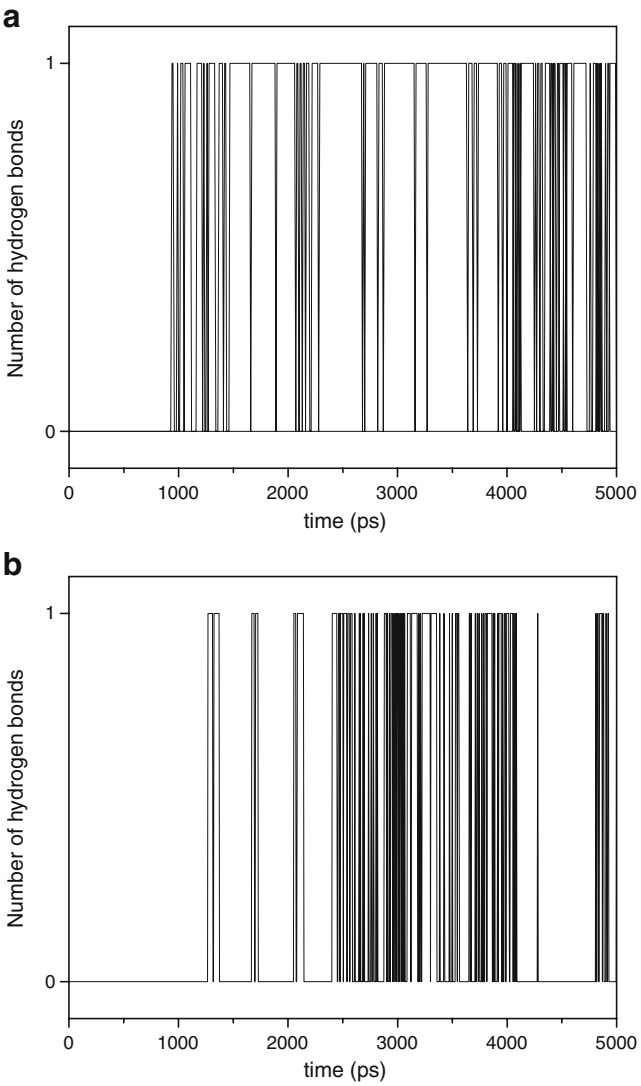

Fig. 5 Hydrogen bonds obtained for compounds **9** (**a**) and **3** (**b**). These interactions are between Ser 141 and the catecholic hydroxyls

the dopamine D2 receptor, the binding site proved to be aligned with aromatic side chains, and such residues can adjust to the different shapes and flexibility of the ligands in the binding site. Thus, Phe 82, Val 83 and Val 87(TM3); Phe 145 (TM5); and Trp 182, Phe 185, Phe 186 and His 189 (TM6) form a mostly hydrophobic pocket for ligands (Fig. 3).

It is interesting to note that the only structural differences between compounds **3**, **6**, **9**, **13** and **16** are the different substituents at C-1. Whereas compound **6** has a relatively rigidly held phenyl ring, the corresponding butyl, benzyl and halogenated-benzyl substituents on compounds **3, 9**, **13** and **16**, respectively, are free to rotate, allowing better accommodation of these hydrophobic moieties to interact with the cluster of aromatic and non polar residues. These results might be better appreciated by observing the different conformational behaviors obtained for the torsional angles of their respective hydrophobic portions during the simulations (Figs. 5–8). The conformational behaviors observed for the torsional angles θ_1 and θ_2 of compound **9** are shown in Fig. 4. Whereas θ_1 is maintained relatively fixed at about 250° during the simulation (Fig. 6a), the torsional angle θ_2 displayed a high molecular flexibility, adopting conformations from 20° to 300° (Fig. 6b). Closely related results were obtained for the torsional angles θ_1 and θ_2 of compounds **13** and **16**. The hydrophobic portion of compound **3**, the butyl moiety, also displayed a high molecular flexibility. Figure 6 gives the conformational behaviors of torsional angles ϕ_1–ϕ_3 of compound **3**. The torsional angle ϕ_1 adopts a relatively rigid planar form close to 170° (Fig. 7a) but the other two torsional angles ϕ_2 and ϕ_3 displayed a high molecular flexibility (Fig. 7b and c, respectively). Very similar results were obtained for the butyl portion of compound **10**. In contrast, the conformational behavior obtained for the phenyl ring of compounds **4**–**6** displayed a very restricted molecular flexibility, keeping a spatial ordering almost perpendicular with respect to the rest of the molecule during the entire simulation (Fig. 8). The different affinities previously reported for compounds **6** and **9** suggest that the orientation of the substituent at C-1 may be a more important factor in the different effects on receptor affinity for the two ligands. This argument also applies to **3**, **10**, **13** and **16**, where the orientations of the butyl and halogenated-benzyl substituents are more favorable for hydrophobic interactions. Thus, the different affinities and selectivities obtained for these compounds might be explained, at least in part, by the different spatial orientations adopted by the varied hydrophobic portions located at C-1, which give different molecular interactions with the D2 receptor. These aspects are discussed in detail in terms of quantum mechanics calculations in the next section.

In the next step of our study, we evaluated the binding energies (BE) obtained for the different complexes. From the binding energies obtained in our MD simulations, one can distinguish a very good binder from a very weak binder (−441,217.42 kJ mol^{-1} for compound **9** vs −441,015.35 kJ mol^{-1} for compound **4**) but cannot distinguish ligands with similar binding affinities (−441,217.42 kJ mol^{-1} for compound **9** vs −441,004.26 kJ mol^{-1} for compound **3** and −441,015.35 kJ mol^{-1} for compound 4 vs −440,155.71 kJ mol^{-1} for compound **1** among other examples). This is not an unexpected result; can we realistically expect to make accurate and reliable predictions with what are decidedly crude representations of the molecular interactions involved in the binding process? Any model that neglects or only poorly approximates the terms that are playing determinant roles, such as, e.g., lone pair directionality in hydrogen bonds, explicit π-stacking polarization effects, hydrogen bonding networks, induced fit, and conformational entropy,

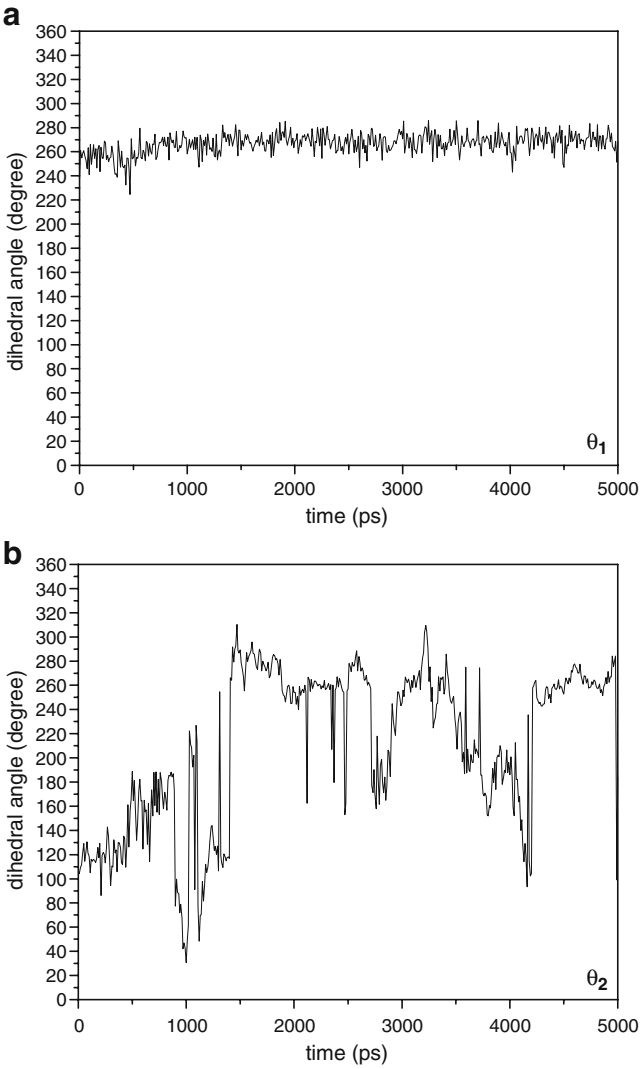

Fig. 6 Evolution of the angles θ_1 (**a**) and θ_2 (**b**) of compound **9** with time during the simulation

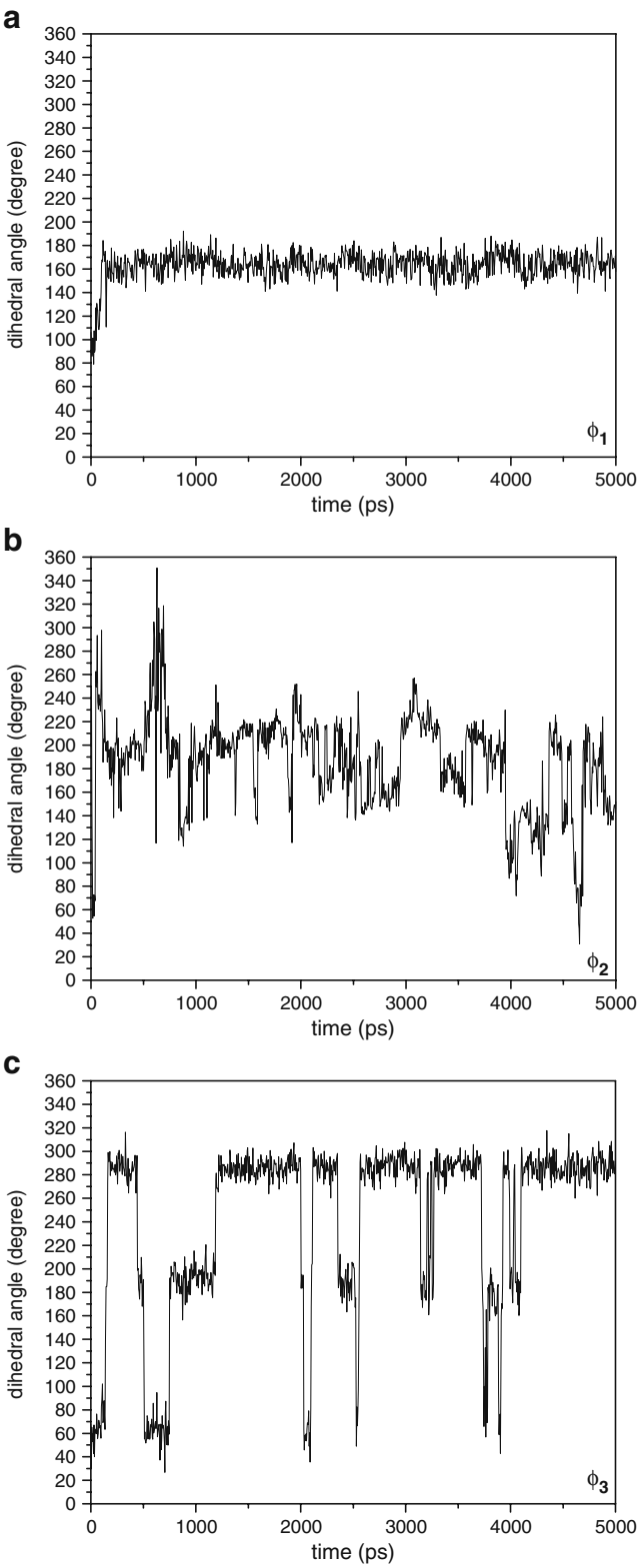

Fig. 7 Evolution of the angles ϕ_1 (**a**), ϕ_2 (**b**) and ϕ_3 (**c**) of compound **3** with time during the simulation

among others, cannot reasonably be expected to distinguish between compounds possessing relatively similar binding

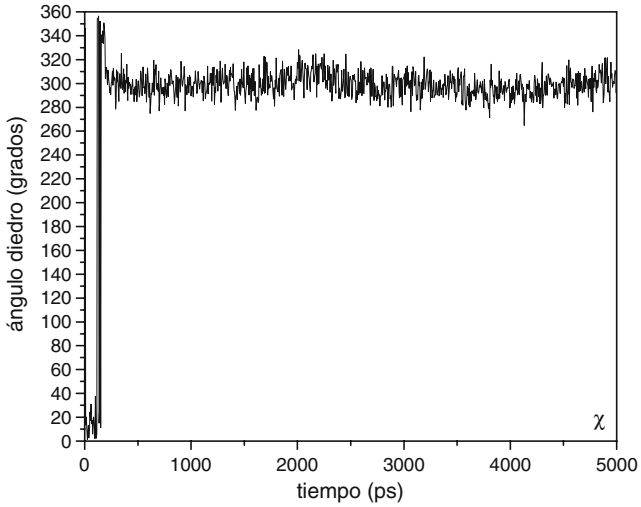

Fig. 8 Evolution of the angle χ of compound **6** with time during the simulation

energies. There are several works supporting this concept in the literature [50, 51].

At this stage of our work, we considered the trend predicted for the MD simulations as certainly significant but, on the other hand, we might be reluctant to assign it a quantitative significance, because of the approximations involved in this mode of approach. It should be noted that we are dealing with relatively weak interactions and therefore MD simulations might underestimate such interactions. Thus, in the next step, we optimized reduced model systems using combined semiempirical, ab initio and DFT calculations.

Quantum mechanics calculations

AM1 calculations combined with RHF/6-31G(d) and DFT [B3LYP/6-31G(d,p)] optimizations were performed by considering all receptor amino acids that could interact after initial positioning of the ligands against Asp 86 and Ser 141 residues. The binding pocket designed in this way (Fig. 3) provided data that matched experimental results previously reported from binding assays [8, 9].

Figure 9a shows ligand **13** interactions with the D2 DR optimized using quantum mechanical calculations. The salt bridge between the protonated amino group and the carboxyl group of Asp 86, as well as the hydrogen bond between the 7-hydroxyl group with Ser 141 can be seen in this figure. From Fig. 9a it is clear that a strong salt bridge exists in this compound between the protonated amino groups and the carboxyl group of Asp 86 (calculated distance of 3.47 Å). The hydrogen bond between **13** and Ser 141 is a bifurcated interaction in which the oxygen atom of the hydroxyl group and the oxygen of carbonyl group of Ser 141 are the proton-acceptors, giving interatomic

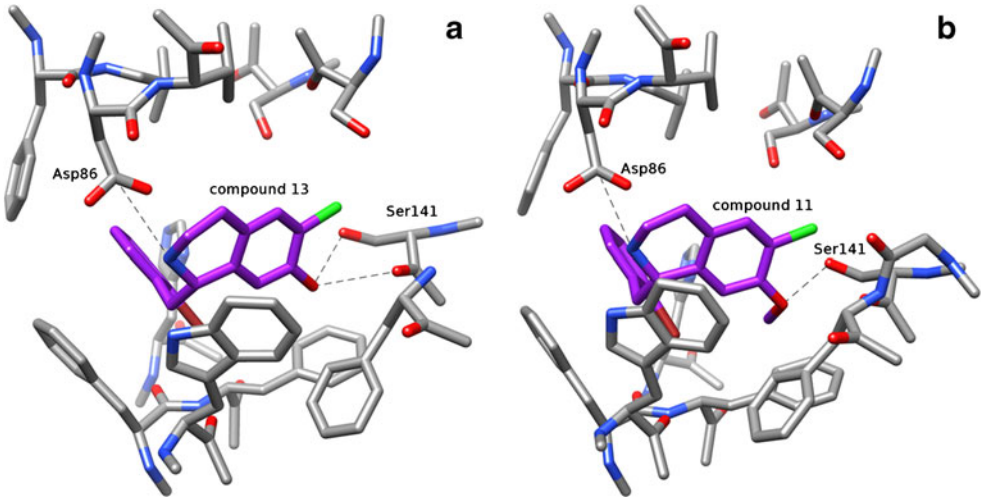

Fig. 9 Interactions of compound **13** (**a**) and **11** (**b**) with the binding pocket of D2 DR. Spatial view of two interactions: salt bridge (Asp 86 with protonated amino group) to the *right* and hydrogen bond between meta-hydroxyl group with Ser 141to the *left*

distances of 2.28 Å and 2.40 Å, respectively. Figure 9b shows ligand **11** interaction with the D2 DR. In this case, the 7-methoxyl group acts as proton-acceptor while the hydroxyl group of Ser 141 is the proton-donor, displaying an interatomic distance of 2.32 Å.

Table 1 gives the BE calculated for the different complexes using RHF/6-31 G(d) and B3LYP/ 6-31 G(d,p) calculations. All compounds possessing 7-methoxyl groups displayed higher BE with respect to the 7- hydroxyl homologues (cf. **1** with **3**; **4** with **6**; **7** with **9**; **11** with **13**, and **14** with **16**). Previously, we reported that a 7-hydroxyl group acting as a proton-donor gives a stronger hydrogen bond than those derivatives possessing a 7-methoxyl group [16]. The present results are in agreement with previously

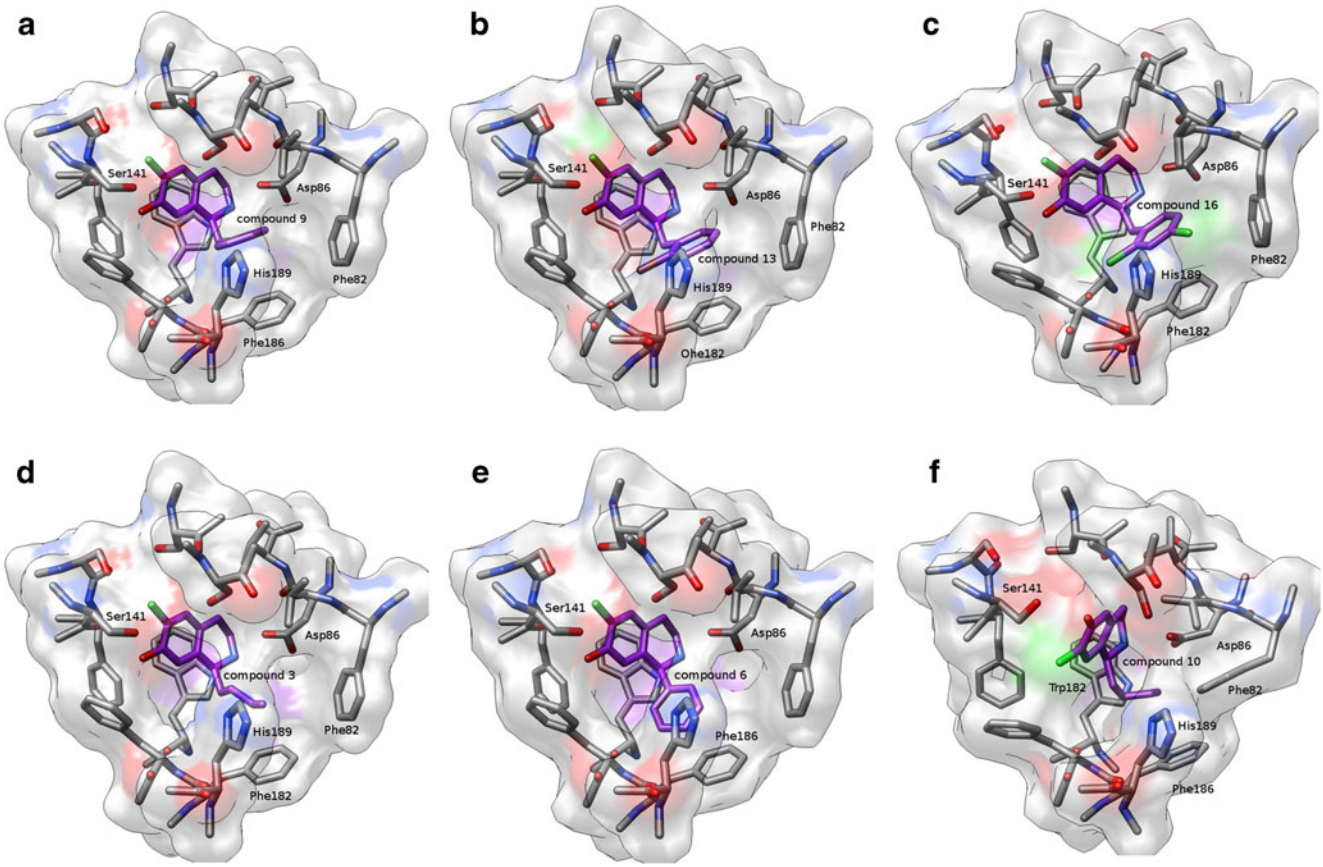

Fig. 10 Interactions of compound **9** (**a**), **13** (**b**), **16** (**c**), **3** (**d**), **6** (**e**) and **10** (**f**) with the binding pocket D2 DR. Different spatial views show the hydrophobic interactions at the hydrophobic zone

reported calculations for isolated and solvated molecules, as well as with previously reported experimental binding affinities [8, 9] (see Table 1).

Figure 10a shows ligand **9** interactions with the binding pocket. In this case, a different spatial view with respect to Fig. 9 is shown in order to better appreciate the hydrophobic interactions. From this figure, we can observe that the benzyl group of **9** adopts an adequate conformation to interact with Phe 186, Phe 82 and His 189. A similar spatial ordering was obtained for compounds **13** and **16** (Fig. 10b and c, respectively). For compounds **13** and **16**, the halogen substituent confers a higher polarizability on the benzyl group, allowing a stronger hydrophobic interaction. In should be noted that compound **13** displayed the highest of p*K*i value in this series. These hydrophobic interactions could explain, at least in part, the strongest affinity obtained for this compound. The butyl group of **3** displays a spatial ordering closely related to that of the benzyl group of **9**, **13** and **16**, also giving closely related hydrophobic interactions with the same hydrophobic residues (Fig. 10d). In contrast, the phenyl group of **6** displayed a different spatial ordering, giving adequate distance to interact only with Phe 186 (Fig. 10e). Interestingly, the bonding energies obtained for these complexes are: **13**/D2 DR < **10**/D2 DR < **9**/D2 DR < **3**/D2 DR < 1**6**/D2 DR, which are in complete agreement with their respective p*K*i values obtained from our previous experimental results (see Table 1). Compound **10** adopts a different spatial ordering at the binding site; thus, the butyl portion of this compound interacts with three aromatic residues: Trp 182, Phe 82 and Phe 186 (Fig. 10f). Compounds **4**–**6** possess a phenyl ring perpendicular to the rest of the ligand from the ring containing the protonated nitrogen [52]. These compounds docked in the D2 receptor model have few interactions in the binding pocket because their 1-phenyl substituents extend toward the extracellular surface of the receptor, parallel to the helix axes. These results are in agreement with those previously reported [23]. Thus, it appears that the shape and flexibility of the side chain at the C-1 position affects the receptor subtype selectivity of ligands to an extent that depends on the geometry, flexibility and stacking potential of ligand substituents. Lan et al. [23], reported that the D1 selective ligand SCH23390 contains a phenyl ring perpendicular to the rest of the molecule and the membrane plane, and parallel to the helix axes, which could explain its selectivity. Our results are in agreement with those results. Compounds type **4**–**6** in this series displayed a conformational behavior closely related to that reported for SCH23390.

Regarding the general structure of BTHIQs reported here, it is reasonable to think that the presence of a chlorine atom at C6, and consequently halogen bonding interactions, could be operative for the ligand–receptor complex formation. Thus, this chlorine possibly could be interacting through either a positive sigma hole with a negative site in its vicinity or through its negative lateral ring of electrostatic potential with a positive site in the vicinity. A comprehensive study on electrostatically driven non-covalent interactions has been reported recently by Politzer et al. [53]. In this latter article, the possibility that halogen and other σ-hole interactions can be competitive with hydrogen bonding has been clearly established. Unfortunately, from the limited information obtained from our relatively low-level theory calculations, it is not possible to properly determine if the halogen bonding interactions could take place here. It is clear that further, more accurate calculations, as well as quantum atoms in molecules (QAIM) [54, 55] analysis are necessary for a detailed description of these interactions. Such calculations are now in progress in our laboratory and will be reported later in a separate paper.

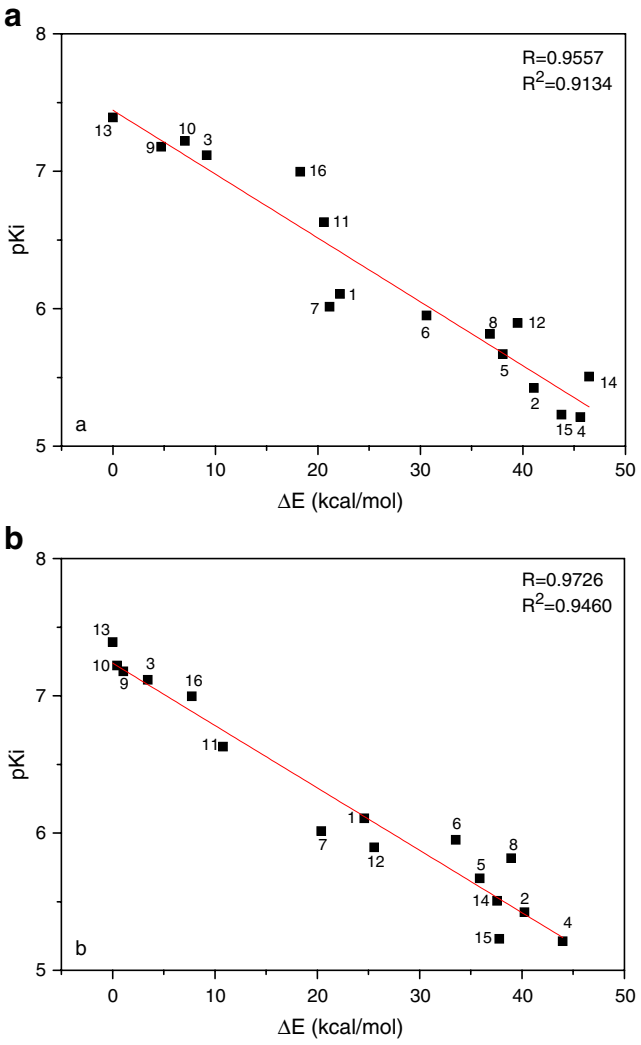

Fig. 11 Correlations obtained between the experimental p*K*i values versus the binding energies (BE) calculated from **a** ab initio [RHF/631G(d)] calculations, and **b** DFT (B3LYP/6-31G(d,p)) computations

Figure 11a gives a graphical representation of the calculated BEs obtained from RHF/6-31G(d) calculations versus experimental p*K*i values, obtained in binding studies in rat striatum [8, 9]. This figure has a correlation coefficient R^2=0.9134. Theisresult is very satisfactory when one considers the type of approximations used. Figure 11b shows the same correlations but in this case using BEs obtained from DFT [B3LYP/6-31G(d,p)] calculations. In this draft, the correlation coefficient is R^2=0.9460 indicating that DFT calculations give a better correlation with the experimental data. Although both linear correlations are good enough to predict the biological activity of BTHIQs, it is clear that DFT calculations give a significantly better correlation with respect to RHF computations. This is particularly evident from the high squares of correlation coefficients, r^2 obtained using RHF and DFT calculations (0.9134 and 0.9460, respectively). From our results, it is clear that the predicted first-principles structure of the primary binding pocket of D2 DR leads to correct predictions of the critical residues for binding THIQs, and gives relative binding affinities that correlate fairly well with those obtained in experiments performed in native tissue. This good correlation provides additional validation for the predicted structure and function.

It should be noted that the AM1 method it is not adequate to describe the hydrogen bonds. In addition, the ab initio and DFT calculations performed here probably do not properly consider the dispersion interactions. Fortunately, in this case it appears that such limitations are not severe enough to prevent us obtaining our objectives. Such an assumption appears to be reasonable, considering the significant correlation obtained between the experimental data and the theoretical calculations performed. However, we cannot exclude that a kind of error-cancellation could have taken place in this case. Thus, it must be pointed out that the approaches used in this study could be operative only for THIQs and structurally related compounds. To extend these approaches to other compounds possessing different structures would require additional validation and more accurate calculations.

Conclusions

A molecular modeling study on 16 BTHIQs acting as dopaminergic ligands was carried out. By combining MD simulations with ab initio and DFT calculations, a simple and generally applicable procedure to evaluate the binding energies of BTHIQs interacting with the D2 DR is reported here, providing a clear picture of the binding interactions of BTHIQs from both structural and energetic viewpoints. Thus, our results give interesting information that may be helpful in obtaining a better understanding of the molecular interactions between BTHIQs and the D2 DR.

A significant correlation between binding energies obtained from DFT calculations and experimental p*K*i values was obtained. These results could predict the potential dopaminergic effect of non-synthesized BTHIQs with an acceptable degree of accuracy. Such information could be essential in determining a priori the putative activity of new BTHIQ derivatives. It is prudent to remark that the excellent correlation obtained here between experimental data and the theoretical calculations performed here could be limited to BTHIQs and structurally related compounds. However, we believe our results may be helpful in the structural identification and understanding of the minimum structural requirements for these molecules, and can provide a guide to the design of BTHIQs with this biological activity.

Acknowledgments Grants from Universidad Nacional de San Luis (UNSL) partially supported this work. This research was also supported by the Spanish "Ministerio de Educación y Ciencia" grant SAF 2007–63142. S.A.A. thanks a postdoctoral fellowship of CONICET-Argentina. R.D.E. is a member of the Consejo Nacional de Investigaciones Científicas y Técnicas (CONICET-Argentina) staff.

References

1. Oloff S, Mailman RB, Tropsha A (2005) Application of validated QSAR models of D1 dopaminergic antagonist for database mining. J Med Chem 48:7322–7332
2. Sit SY, Xie K, Jacutin-Porte S, Boy KM, Seanz J, Taber MT, Gulwadi AG, Korpinen CD, Burris KD, Molski TF, Ryan E, Xu C, Verdoorn T, Johnson G, Nichols DE, Mailman RB (2004) Synthesis and SAR exploration of dinapsoline analogues. Bioorg Med Chem 12:715–734
3. Strange PG (1997) Dopamine receptors. Tocris Reviews 15. Tocris Cookson, Bristol
4. Zhang A, Neumeyer JL, Baldessarini RJ (2007) Recent progress in development of dopamine receptor subtype-selectiveagents: potential therapeutics for neurological and psychiatric disorders. Chem Rev 107:274–302
5. Protais P, Arbaoui J, Bakkali EH, Bermejo A, Cortes D (1995) Effects of various isoquinoline alkaloids on in vitro ^{3}H-dopamine uptake. J Nat Prod 58:1475–1484
6. Bermejo A, Protais P, Blázquez MA, Rao KS, Zafra-Polo MC, Cortes D (1995) Dopaminergic isoquinoline alkaloids from rotos of *Xylopia papuana*. Nat Prod Res 6:57–62
7. Cabedo N, Protais P, Cassels BK, Cortes D (1998) Synthesis and dopamine receptor selectivity of the benzyltetrahydroisoquinoline, (*R*)-(+)-*nor*-roefractine. J Nat Prod 61:709–712
8. Cabedo N, Andreu I, Ramírez de Arellano MC, Chagraoui A, Serrano A, Bermejo A, Protais P, Cortes D (2001) Enantioselective syntheses of dopaminergic (*R*)- and (*S*)-benzyltetrahydroisoquinolines. J Med Chem 44:1794–1801
9. Berenguer I, El Aouad N, Andujar S, Romero V, Suvire F, Freret T, Bermejo A, Ivorra MD, Enriz RD, Boulouard M, Cabedo N, Cortes D (2009) Tetrahydroisoquinolines as dopaminergic ligands: 1-butyl-7-chloro-6-hydroxy-tetrahydroisoquinoline, a new compound with antidepressant-like activity in mice. Bioorg Med Chem 17:4968–4980
10. El Aouad N, Berenguer I, Romero V, Marín P, Serrano A, Andujar S, Suvire F, Bermejo A, Ivorra MD, Enriz RD, Cabedo N, Cortes

D (2009) Structure–activity relationship of dopaminergic halogenated 1-benzyl-tetrahydroisoquinoline derivatives. Eur J Med Chem 44:4616–4621
11. Andreu I, Cabedo N, Torres G, Chagraoui A, Ramirez de Arellano MC, Gil S, Bermejo A, Valpuesta M, Portais P, Cortes D (2002) Syntheses of dopaminergic 1-cyclohexylmethyl-78-dioxygenated tetrahydroisoquinolines by selective heterogeneous tandem hydrogenation. Tetrahedron 58:10173–10179
12. Bermejo A, Andreu I, Suvire F, Léonce S, Caignard DH, Renard P, Pierré A, Enriz RD, Cortes D, Cabedo N (2002) Syntheses and antitumor targeting G1 phase of the cell cycle of benzoyldihydroisoquinoline. J Med Chem 45:5058–5068
13. Suvire FD, Andreu I, Bermejo A, Zamora MA, Cortes D, Enriz RD (2003) Conformational study of *N*-alkyl-benzyltetrahydroisoquinolines alkaloid. J Mol Struct THEOCHEM 666–667:109–116
14. Suvire FD, Cabedo N, Chagraoui A, Zamora MA, Cortes D, Enriz RD (2003) Molecular recognition and binding mechanism of *N*-alkyl-benzyltetrahydro-isoquinolines to the D_1 dopamine receptor. A computational approach. J Mol Struc THEOCHEM 666–667:455–467
15. Andreu I, Cortes D, Protais P, Cassels BK, Chagraoui A, Cabedo N (2000) Preparation of dopaminergic *N*-Alkyl-benzyltetrahydroisoquinolines using a 'One-Pot' procedure in acid medium. Bioorg Med Chem 8:889–895
16. Doi S, Shirai N, Sato Y (1997) Abnormal products in the Bischler-Napieralski isoquinoline synthesis. J Chem Soc Perkin Trans 1:2217–2221
17. Andujar SA, Migliore de Angel BM, Charris JE, Israel A, Suárez-Roca H, López SE, Garrido MR, Cabrera EV, Visual G, Rosales C, Suvire FD, Enriz RD, Angel-Guío JE (2008) Synthesis dopaminergic profile and molecular dynamics calculations of N-aralkyl substituted 2-aminoindans. Bioorg Med Chem 16:3233–3244
18. Kalani MYS, Vaidehi N, Hall SE, Trabanino RJ, Freddolino PL, Kalani MA, Floriano WB, Wai Tak Kam V, Goddard WA III (2005) The predicted 3D structure of the human D2 dopamine receptor and the binding site and binding affinities for agonists and antagonists. Proc Natl Acad Sci USA 101:3815–3820
19. Becker OM, Marantz Y, Shacham S, Inbal B, Heifetz A, Kalid O, Bar-Haim S, Warshaviak D, Fichman M, Noiman SG (2004) Protein-coupled receptors: in silico drug discovery in 3D. Proc Natl Acad Sci USA 101:11304–11309
20. Micheli F, Bonanomi G, Blaney FE, Braggio S, Capelli AM, Checchia A, Curcuruto O, Damiani F, Di Fabio R, Donati D, Gentile G, Gribble A, Hamprecht D, Tedesco G, Terreni S, Tarsi L, Lightfoot A, Stemp G, MacDonald G, Smith A, Pecoraro M, Petrone M, Perini O, Piner J, Rossi T, Worby A, Pilla M, Valerio E, Griffante C, Mugnaini M, Wood M, Scott C, Andreoli M, Lacroix L, Schwarz A, Gozzi A, Bifone A, Ashby CR Jr, Hagan JJ, Heidbreder C (2007) 124-Triazol-3-yl-thiopropyl-tetrahydrobenzazepines: a series of potent and selective dopamine D3 receptor antagonists. J Med Chem 50:5076–5089
21. Ribeiro AA, Horta BAC, de Alencastro RB (2008) MKTOP: a program for automatic construction of molecular topologies. J Braz Chem Soc 19:1433–1435
22. Manzour A, Meng F, Meador-Woodruff JH, Taylor LP, Civelli O, Akil H (1992) Site-directed mutagenesis of the human dopamine D_2 receptor. Eur J Pharm Mol Pharmacol Sec 227:205–214
23. Lan H, DuRand CJ, Teeter MM, Neve KA (2006) Structural determinants of pharmacological specificity between D_1 and D_2 dopamine receptors. Mol Pharmacol 69:185–194
24. Berendsen HJC, Van der Spoel D, Van Drunen R (1995) GROMACS: a message-passing parallel molecular dynamics implementations. Comput Phys Commun 91:43–56
25. Lindahl E, Hess B, van der Spoel D (2001) GROMACS 3.0: a package for molecular simulations and trajectory analysis. J Mol Model 7:306–317
26. van Buuren AR, Marrink SJ, Berendsen HJC (1993) A molecular dynamics study of the decane/water interface. J Phys Chem 36:9206–9212
27. Mark AE, van Helden SP, Smith PE, Janssen LHM, van Gunsteren WF (1994) Convergence properties of free energy calculations. A-cyclodextrin complexes as a case study. J Am Chem Soc 116:6293–6302
28. Jorgensen WL, Chandrasekhar J, Madura JD, Impey RW, Klein ML (1983) Comparison of simple potential functions for simulating liquid water. J Chem Phys 79:926–935
29. van Buuren AR, Berendsen HJC (1993) Molecular dynamics simulation of the stability of a 22 residue alpha-helix in water and 30% trifluoroethanol. Biopolymers 33:1159–1166
30. Liu H, Muller-Plathe F, van Gunsteren WF (1995) A force field for liquid dimethyl sulfoxide and physical properties of liquid dimethyl sulfoxide calculated using molecular dynamics simulation. J Am Chem Soc 117:4363–4366
31. Miyamoto S, Kollman PA (1992) SETTLE—an analytical version of the SHAKE and RATTLE algorithm for rigid water models. J Comput Chem 13:952–962
32. Berendsen HJC, Postma HJC, Van Gunsteren WF, Hermans WF (1981) Interaction models for water in relation to protein hydration. In: Pullman B (ed) Intermolecular forces. Reidel, Dordrecht, pp 331–342
33. Darden T, York D, Pedersen L (1993) Particle mesh Ewald—an N. log(n) method for Ewald sums in large systems. J Chem Phys 98:10089–10092
34. Essmann U, Perera L, Berkowitz ML, Darden T, Lee H, Pedersen LG (1995) A smooth particle mesh Ewald method. J Chem Phys 103:8577–8593
35. Luty B, Tironi IG, van Gunsteren WF (1995) Lattice–sum methods for calculating electrostatic interactions in molecular simulations. J Chem Phys 103:3014–3021
36. Zimmerman K (1991) All purpose molecular mechanics simulator and energy minimizer. J Comput Chem 12:310–319
37. Ferguson DM (1995) Parameterization and evaluation of a flexible water model. J Comput Chem 16:501–511
38. Berendsen HJC, Postma JPM, DiNola A, Haak JR (1984) Molecular dynamics with coupling to an external bath. J Chem Phys 81:3684–3690
39. Hess B, Bekker H, Berendsen HJC, Fraaije JG (1997) E.M. LINCS: a linear constraint solver for molecular simulations. J Comput Chem 18:1463–1472
40. Kampmann T, Mueller DS, Mark AE, Young PR, Kobe B (2006) The role of histidine residues in low-pH-mediated viral membrane fusion. Structure 14:1481–1487
41. Teeter MM, Froimowitz MF, Stec B, Durand CJ (1994) Homology modeling of the dopamine D2 receptor and its testing by docking of agonists and tricyclic antagonists. J Med Chem 37:2874–2888
42. Neve KA, Cumbay MG, Thompson KR, Yang R, Buck DC, Watts VJ, Durand CJ, Teeter MM (2001) Modeling and mutational analysis of a putative sodium-binding pocket on the dopamine D_2 receptor. Mol Pharmacol 60:373–381
43. Frisch MJ, Trucks GW, Schlegel HB, Scuseria GE, Robb MA, Cheeseman JR, Montgomery JA Jr, Vreven T, Kudin KN, Burant JC, Millam JM, Iyengar SS, Tomasi J, Barone V, Mennucci B, Cossi M, Scalmani G, Rega N, Petersson GA, Nakatsuji H, Hada M, Ehara M, Toyota K, Fukuda R, Hasegawa J, Ishida M, Nakajima T, Honda Y, Kitao O, Nakai H, Klene M, Li X, Knox JE, Hratchian HP, Cross JB, Adamo C, Jaramillo J, Gomperts R, Stratmann RE, Yazyev O, Austin AJ, Cammi R, Pomelli C, Ochterski JW, Ayala PY, Morokuma K, Voth GA, Salvador P, Dannenberg JJ, Zakrzewski VG, Dapprich S, Daniels AD, Strain MC, Farkas O, Malick DK, Rabuck AD, Raghavachari K, Foresman JB, Ortiz JV, Cui Q, Baboul AG, Clifford S, Cioslowski

J, Stefanov BB, Liu G, Liashenko A, Piskorz P, Komaromi I, Martin RL, Fox DJ, Keith T, Al-Laham MA, Peng CY, Nanayakkara A, Challacombe M, Gill PMW, Johnson B, Chen W, Wong MW, Gonzalez C, Pople JA (2003) Gaussian 03, Revision B.05. Gaussian Inc, Pittsburgh

44. Pettersen EF, Goddard TD, Huang CC, Couch GS, Greenblatt DM, Meng EC, Ferrin TE (2004) UCSF Chimera—a visualization system for exploratory research and analysis. J Comput Chem 25:1605–1612
45. Hjerde E, Dahl SG, Sylte I (2005) Atypical and typical antipsychotic drug interactionswith the dopamine D_2 receptor. Eur J Med Chem 40:185–194
46. Cho W, Taylor LP, Mansour A, Akil A (1995) Hydrophobic residues of the D_2 dopamine receptor are important for binding and signal transduction. J Neurochem 65:2105–2115
47. Cox BA, Henningsen RA, Spanoyannis A, Neve RL, Neve KA (1992) Contributions of conserved serine residues to the interactions of ligands with dopamine D_2 receptors. J Neurochem 59:627–635
48. Wiens BL, Nelson CS, Neve KA (1998) Contribution of serine residues to constitutive and agonist-induced signaling via the D2Sdopamine receptor: evidence for multiple agonist-specific active conformations. Mol Pharmacol 54:435–444
49. Wilcox RE, Huang WH, Brusniak MYK, Wilcox DM, Pearlman RS, Teeter MM, Durand CJ, Wiens BL, Neve KA (2000) CoMFA-based prediction of agonist affinities at recombinant wild type versus serine to alanine point mutated D_2 dopamine receptors. J Med Chem 43:3005–3019
50. Page CS, Bates PA (2008) Can MM-PBSA calculations Predict the specifiicties of protein kinase inhibitors? J Comput Chem 27:1990–2007
51. Mertz KM (2010) Limits of free energy computation for protein–ligand interactions. J Chem Theor Comput 6:1769–1776
52. Breneman CM, Wiberg KB (1990) Determining atom-centered monopoles from molecular electrostatic potentials. The need for high sampling density in formamide conformational analysis. J Comput Chem 11:361–373
53. Politzer P, Murray JS, Clark T (2010) Halogen bonding: an electrostatically-driven highly directional noncovalent interaction. Phys Chem Chem Phys 12:7748–7757
54. Bader RFW (1990) Atoms in molecules. A quantum theory. Oxford University Press, Oxford
55. Popelier PLA (1999) Atoms in molecules. An introduction. Pearson, Harlow